Buletinul Ştiinţific al Universităţii "Politehnica" din Timişoara

Seria ELECTRONICĂ şi TELECOMUNICAŢII
TRANSACTIONS on ELECTRONICS and COMMUNICATIONS

Tom 56(70), Fascicola 1, 2011

CMOS Wilson-Widlar Total-Current Temperature Sensor

Bogdan V. Marinca[1]

Abstract: - This paper describes a new integrated-on-silicon circuit, made of two cross-connected classical current mirrors. This temperature sensor can be seen in the first place by a simple interconnection, serial with the load resistance, and good sensitivity and linearity. We analyze the performance of this scheme for different types of used integrated resistors, with positive, zero and negative temperature coefficient. It highlighted the possibility of achieving a better overall performance when using a combination of NTC and PTC resistors type. We followed the maximal variation of total output current with temperature. A design with maximum slope is presented, having an error of 4.05% between analytical and simulated slope. Sensor performances are improved: 0.514%/°C percentage slope, low power consumption of 42.9µA at 20°C, supply regulation parameter of 7897ppm/V at 3.5V and a total variation of percentage slope with process of only 3.66%.

Keywords: CMOS temperature sensor, total-current temperature sensor, use of NTC, PTC, ZTC resistors

I. INTRODUCTION

The aim of this paper is to design a simple temperature sensor in 0.35µm technology, whose output current is strongly dependent on temperature. It is implemented with CMOS transistors and the latest generation of integrated resistances whose temperature coefficient of order I and II are known. These resistors can be themselves used as temperature sensors, but present some disadvantages: the current trough them depends on voltage supply and the process variation is 30% in comparison with 3.66% for the presently proposed circuit.

For the implementation of the above mentioned temperature sensor we propose a mix of cross-connected classical mirrors. They involve a combination of a modified Wilson mirror and a normal Widlar mirror (Fig. 1). Modified Wilson mirror provides a good branch-current variation and total-current variation with temperature for a certain value and certain type of resistance which replaces the diode. Also it is simpler than modified Widlar mirror (with 4 parts). The Wilson-mirror proposed sensor can provide a good Supply Regulation (SR) parameter and relatively low sensitivity to process thanks to the negative feedback.

The calculation of first and second-order temperature coefficients for the branch-current ratio *m,* is presented in Section 2. Section 3 is a mathematical analysis of the variation of total-current slope and will be compared with the simulation and optimization results presented in Section 4. Section 5 includes the measures of the percentage slope and current variations with the process while Section 6 shows the conclusions of that paper.

II. CALCULATION OF FIRST AND SECOND ORDER TEMPERATURE COEFFICIENTS

It is analysed the total-current dependence with the temperature, starting from a standard current source. The circuit shown in Fig. 1 is made from a simple upper mirror (the M_3 and M_4) and a lower modified Wilson mirror (with M_1, M_2 and R_1). Also, the ratio m of the two branch currents is temperature dependent.

From the 0.35µm technology process specification the following 5V-transistors parameters can be extracted: carrier_mobility $\mu_n=388\cdot10^{-4}$ [m²/Vs], $\mu_p=215\cdot10^{-4}$ [m²/Vs], $\varepsilon_{ox}=3{,}45\cdot10^{-11}$ [F/cm], $t_{ox}=11\cdot10^{-9}$ [m].

The threshold-voltage temperature coefficient, k_{VTn} (having V_{Tn}=0,82V for 5V NMOS transistors), is determined as follows:

$$k_{VTn}=\frac{1}{V_{Tn}}\cdot\frac{dV_{Tn}}{dT} \qquad (1)$$

where the derivative of threshold voltage value with temperature is given in the process specification model list for used transistor and is negative ($-1{,}5\cdot10^{-3}$ [1/K]). k_{VTnVTn} is the second order threshold voltage temperature coefficient and is defined by:

$$k_{VTnVTn}=\frac{dk_{VTn}}{dT} \qquad (2)$$

The study of the ratio m dependency with temperature for a simple mirror, connected in the upper part of the circuit, has been made by simulation (Fig. 3). Temperature range in these simulations has been -30 to 120°C. The first-order temperature coefficient of the m ratio is:

[1] Facultatea de Electronică şi Telecomunicaţii, Departamentul Electronică Aplicată Bd. V. Pârvan Nr. 2, 300223 Timişoara, e-mail: bogdan.marinca@etc.upt.ro

$$k_m = \frac{\dfrac{I_{2[120^\circ C]}}{I_{1[120^\circ C]}} - \dfrac{I_{2[-30^\circ C]}}{I_{1[-30^\circ C]}}}{120-(-30)} = \qquad (3)$$

$$= 0.10595 \cdot 10^{-3} [\frac{1}{K}]$$

The second-order temperature coefficient of branch-current ratio, k_{mm} , is defined similarly with the (2) equation.

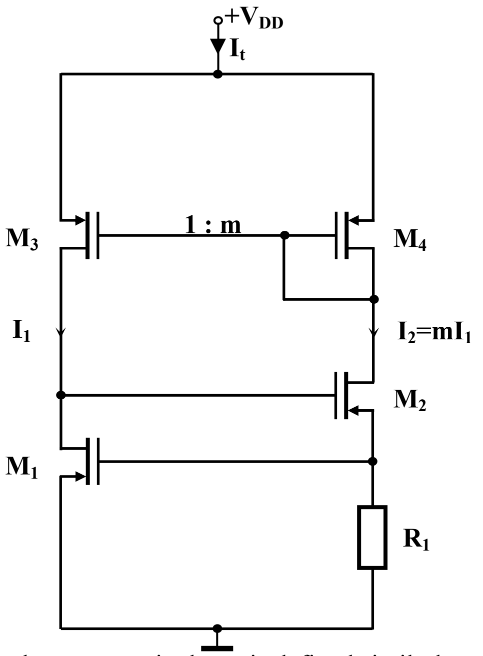

Fig.1. Wilson-simple mirror total-current temperature sensor.

The temperature coefficient of integrated resistors k_R is directly extracted from the list of process specification parameters model. If it is necessary to achieve lower manufacturing dispersion is recommended PTC type: "N+ diffusion sheet resistance" which has typical value of 90Ω/□, first-order temperature coefficient k_R=+1,6•10^{-3}/K, and zero second-order temperature coefficient [1]. In some cases, in order to improve nonlinearity slope and optimize certain parameters, it is recommended to use a NTC type resistance: "N+ UG Polysilicon 1 sheet resistance", with high typical square value (1000Ω/□), and small area on chip. For this, the first-order temperature coefficient is negative: k_R=-2.84•10^{-3}/K, and the second-order coefficient has positive value: k_{RR} = +7,36·10^{-6} /K^2 [1].

The carrier-mobility temperature coefficient $k_{\mu n}$ for NMOS transistor can be find in the 5V CMOS 0.35μm technology transistor data sheet. The "temperature exponent" for β_n gain factor is extracted from the parameters' table. It is noted BEX and is used the mobility temperature dependence equation:

$$\ln \mu_n(T) = \ln \mu_n(T_o) + BEX[\ln T - \ln T_o] \qquad (4)$$

So, the mobility equation and $k_{\mu n}$ become:

$$\mu_n(T) = \mu_n(T_o) \cdot e^{BEX[\ln(T)-\ln(To)]} \qquad (5)$$

$$k_{\mu_n} = \frac{d\mu_n}{\mu_n dT} = \frac{1}{\mu_n(T)} \mu_n(T_o) BEX \frac{1}{T} e^{BEX \ln\frac{T}{T_o}} = \frac{BEX}{T} \qquad (6)$$

The above equation shows that $k_{\mu n}$ depends nonlinearly by the temperature. For a temperature range between 240 to 400 K $k_{\mu n}$ have the shape variation presented in Fig. 2 [1].

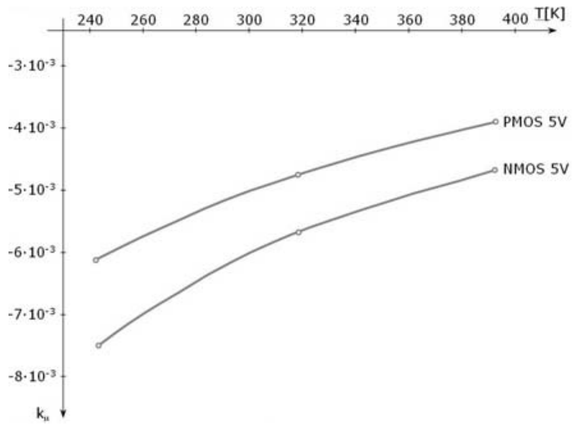

Fig.2. k_μ versus temperature for 5V transistors.

The expressions of temperature coefficients k_μ for 5V model can be derived by linear approximation from the graph below [1]:

$$k_{\mu p} = [-5.43 + 0.0148(T-273)] \cdot 10^{-3} [1/K] \quad (7)$$

$$k_{\mu n} = [-6.53 + 0.0177(T-273)] \cdot 10^{-3} [1/K] \quad (8)$$

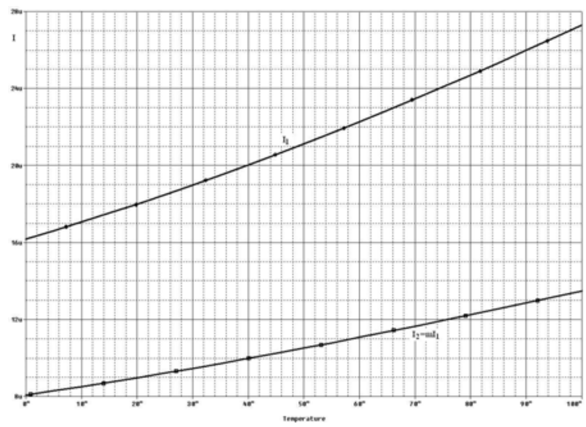

Fig.3. Variation of branch currents versus temperature in a simple current mirror

III. THE DETERMINATION OF THE MAXIMUM SLOPE

For estimate the temperature dependence of the sensor, the total-current variation versus temperature (sensor sensitivity) is calculated and maximized. Total-current relationship can be obtained starting from the one written on the bottom loop of the cell:

$$V_{GS1}=I_2\cdot R_1=m\cdot I_1\cdot R_1 \text{ or } V_{Tn}+\sqrt{\frac{I_1}{\beta_m\cdot\alpha_1}}=m\cdot I_1\cdot R_1 \quad (9)$$

This yelds:

$$\frac{m}{1+m}\cdot R_1\cdot I_t-\sqrt{\frac{I_t}{(1+m)\cdot\beta_n\cdot\alpha_1}}-V_{Tn}=0 \quad (10)$$

where m is the current ratio (I_2=mI_1); I_t is the total-current (I_t=I_1+I_2); $\beta_n=\mu_n\cdot C_{ox}/2$ is the gain factor of NMOS transistors (the same for all, regardless of size), α_1 is the dimensional ratio W_1/L_1 of transistor M_1, and V_{Tn} is the threshold voltage of NMOS transistors (considered to be the same for all, regardless of size). So, we can write the next relation:

$$I_t=I_1+mI_1=(1+m)I_1 \quad (11)$$

Using the expression of β_n and the notation $U=\mu_n\cdot C_{ox}\cdot\alpha_1$, we obtain :

$$I_t^2-2\cdot I_t\left(\frac{m+1}{m}\cdot\frac{V_{Tn}}{R_1}+\frac{m+1}{m^2\cdot R_1^2\cdot U^2}\right)+\left(\frac{m+1}{m}\right)^2\cdot\frac{V_{Tn}^2}{R_1^2}=0 \quad (12)$$

The solutions of equation (12) are:

$$I_{t\,1,2}=\frac{m+1}{m}\cdot\frac{V_{Tn}}{R_1}+\frac{m+1}{m^2\cdot R_1^2\cdot U}\pm \pm\sqrt{\frac{1}{m^2\cdot R_1^2\cdot U^2}+\frac{2\cdot V_{Tn}}{m\cdot R_1\cdot U}}\cdot\frac{m+1}{m\cdot R_1} \quad (13)$$

We introduce now the notations:

$$X=\sqrt{\frac{1}{m^2\cdot R_1^2\cdot U^2}+\frac{2\cdot V_{Tn}}{m\cdot R_1\cdot U}} \quad (14)$$

$$A=\frac{k_{VTn}-k_m-k_{R_1}-k_{\mu n}}{m\cdot R_1\cdot U}\cdot V_{Tn}-\frac{k_m+k_{R_1}+k_{\mu n}}{m^2\cdot R_1^2\cdot U^2}$$

and the total-current slope definition:

$$P=\frac{dI_t}{dT} \quad (15)$$

Now, the slopes are:

$$P_{1,2}=\frac{(m+1)\cdot(k_{VTn}-k_{R1})-k_m}{m}\cdot\frac{V_{Tn}}{R_1}-\frac{(m+1)\cdot(2\cdot k_{R_1}+k_{\mu n})+(m+2)\cdot k_m}{m^2\cdot R_1^2\cdot U}\pm \pm\{\frac{m+1}{m\cdot R_1\cdot X}A-\frac{k_m+(m+1)\cdot k_{R_1}}{m\cdot R_1}\cdot X\} \quad (16)$$

To have the maximum slope it is necessary that the derivative of slopes in relation with temperature to be null:

$$\frac{d}{dT}\left(P_{1,2}\right)=0 \quad (17)$$

$$\frac{d}{dT}\cdot\left[\frac{(m+1)\cdot(k_{V_{Tn}}-k_{R_1})-k_m}{m}\cdot\frac{V_{Tn}}{R_1}\right]= =\frac{k_m^2-k_{mm}+2k_m(k_{R_1}-k_{V_{Tn}})}{m\cdot R_1}\cdot V_{Tn}+ +\frac{(m+1)\cdot\left[\left(k_{V_{Tn}}-k_{R_1}\right)^2+k_{V_{Tn}V_{Tn}}-k_{R_1R_1}\right]}{m\cdot R_1}\cdot V_{Tn} \quad (18)$$

$$\frac{d}{dT}\cdot\left[\frac{(m+1)\cdot(2\cdot k_{R_1}+k_{\mu n})+(m+2)\cdot k_m}{m^2\cdot R_1^2\cdot U}\right]= =\frac{(m+2)\cdot k_{mm}}{m^2\cdot R_1^2\cdot U}+ +\frac{(m+1)\cdot\left[2\cdot k_{R_1R_1}+k_{\mu n\mu n}-(2\cdot k_{R_1}+k_{\mu n})^2\right]}{m^2\cdot R_1^2\cdot U}- -\frac{(m+4)\cdot k_m^2-2\cdot(m+2)\cdot k_m\cdot(2\cdot k_{R_1}+k_{\mu n})}{m^2\cdot R_1^2\cdot U} \quad (19)$$

$$\frac{d}{dT}\cdot\left\{\frac{m+1}{m\cdot R_1\cdot X}\cdot A\right\}= =\frac{m+1}{m\cdot R_1\cdot X}\cdot[\frac{k_{V_{Tn}V_{Tn}}-k_{mm}-k_{R_1R_1}-k_{\mu n\mu n}}{m\cdot R_1\cdot U}+ +\frac{(k_m+k_{R_1}+k_{\mu n}-k_{V_{Tn}})^2}{m\cdot R_1\cdot U}\cdot V_{Tn}+ +\frac{2\cdot(k_m+k_{R_1}+k_{\mu n})^2-k_{mm}-k_{R_1R_1}-k_{\mu n\mu n}}{m^2\cdot R_1^2\cdot U^2}]-$$

$$-\frac{k_m+(m+1)\cdot k_{R_1}}{m\cdot R_1\cdot X}\cdot\Big[\frac{(k_{V_{Tn}}-k_m-k_{R_1}-k_{\mu n})\cdot V_{Tn}}{m\cdot R_1\cdot U}-\frac{k_m+k_{R_1}+k_{\mu n}}{m^2\cdot R_1^2\cdot U^2}\Big]-\frac{m+1}{m\cdot R_1\cdot X^3}\cdot\left[\frac{(k_{V_{Tn}}-k_m-k_{R_1}-k_{\mu n})\cdot V_{Tn}}{m\cdot R_1\cdot U}-\frac{k_m+k_{R_1}+k_{\mu n}}{m^2\cdot R_1^2\cdot U^2}\right]^2 \quad (20)$$

$$\frac{d}{dT}\cdot\left[\frac{k_m+(m+1)\cdot k_{R_1}}{m\cdot R_1}\cdot X\right]=$$
$$=\frac{k_{mm}+(m+1)\cdot k_{R_1R_1}-(m+1)\cdot k_{R_1}^{\ 2}}{m\cdot R_1}\cdot X-$$
$$-\frac{-k_m^2-2\cdot k_m\cdot k_{R_1}}{m\cdot R_1}\cdot X+\frac{k_m+(m+1)\cdot k_{R_1}}{m\cdot R_1\cdot X}\cdot$$
$$\cdot\left[\frac{(k_{V_{Tn}}-k_m-k_{R_1}-k_{\mu n})\cdot V_{Tn}}{m\cdot R_1\cdot U}-\frac{k_m+k_{R_1}+k_{\mu n}}{m^2\cdot R_1^2\cdot U^2}\right] \quad (21)$$

From equations (18), (19), (20) and (21) the condition of maximum slope is obtained:

$$\frac{k_m^2-k_{mm}+2\cdot k_m\cdot(k_{R_1}-k_{V_{Tn}})}{m\cdot R_1}\cdot V_{Tn}+$$
$$+\frac{(m+1)\cdot\left[(k_{V_{Tn}}-k_{R_1})^2+k_{V_{Tn}V_{Tn}}-k_{R_1R_1}\right]}{m\cdot R_1}\cdot V_{Tn}+$$
$$+\frac{(m+1)\cdot\left[(2\cdot k_{R_1}+k_{\mu n})^2-2\cdot k_{R_1R_1}-k_{\mu n\mu n}\right]}{m^2\cdot R_1^{\ 2}\cdot U}$$
$$-\frac{(m+2)\cdot k_{mm}}{m^2\cdot R_1^{\ 2}\cdot U}+$$
$$+\frac{(m+4)\cdot k_m^2+2\cdot(m+2)\cdot k_m(2\cdot k_{R_1}+k_{\mu n})}{m^2\cdot R_1^{\ 2}\cdot U}\pm$$
$$\pm\{\frac{m+1}{m\cdot R_1\cdot X}\cdot[\frac{k_{V_{Tn}V_{Tn}}-k_{mm}-k_{R_1R_1}-k_{\mu n\mu n}}{m\cdot R_1\cdot U}\cdot V_{Tn}+$$
$$+\frac{(k_m+k_{R_1}-k_{V_{Tn}})^2}{m\cdot R_1\cdot U}\cdot V_{Tn}+$$
$$+\frac{2\cdot(k_m+k_{R_1}+k_{\mu n})^2-k_{mm}-k_{R_1R_1}-k_{\mu n\mu n}}{m^2\cdot R_1^{\ 2}\cdot U^2}]-$$
$$-\frac{2\cdot[k_m+(m+1)\cdot k_{R_1}]}{m\cdot R_1\cdot X}\cdot\frac{(k_{V_{Tn}}-k_m-k_{R_1}-k_{\mu n})\cdot V_{Tn}}{m\cdot R_1\cdot U}+$$
$$-\frac{2\cdot[k_m+(m+1)\cdot k_{R_1}]}{m\cdot R_1\cdot X}\cdot\frac{(k_{V_{Tn}}-k_m-k_{R_1}-k_{\mu n})\cdot V_{Tn}}{m\cdot R_1\cdot U}+$$
$$+\frac{2\cdot\lfloor k_m+(m+1)\cdot k_{R_1}\rfloor}{m\cdot R_1\cdot X}\cdot\frac{k_m+k_{R_1}+k_{\mu n}}{m^2\cdot R_1^{\ 2}\cdot U^2}-$$
$$-\frac{m+1}{m\cdot R_1\cdot X^3}\left[\frac{(k_{V_{Tn}}-k_m-k_{R_1}-k_{\mu n})\cdot V_{Tn}}{m\cdot R_1\cdot U}-\frac{k_m+k_{R_1}+k_{\mu n}}{m^2\cdot R_1^{\ 2}\cdot U^2}\right]^2+$$
$$+\frac{k_m^2+(m+1)\cdot(k_{R_1}^2-k_{R_1R_1})+2\cdot k_m\cdot k_{R_1}-k_{mm}}{m\cdot R_1}\cdot X\}=0 \quad (22)$$

Substituting the values of the temperature coefficients in equation (22) and taking into account the values of the components obtained by performing simulations we calculate the total-current slope of the sensor using the relation given by (16).

Simulations were made for different values of R_1 between 10kΩ and 140kΩ, and for different types of resistance: PTC, NTC and ZTC.

Table 1: Results of total-current slope calculation

R_1 Sheet Resist.	PTC			ZTC	NTC	
	Poly-silicon 1	*N+ Diffusion*	*N-Well*	*LOW TCR Poly-silicon 2*	*N^+UG Poly-silicon 1*	*P^+UG Poly-silicon 1*
Slope [μA/ºC]	-0.0002	-0.0024	-0.0001	0.0401	0.1520	0.0515

The maximum analytical total-current slope is obtained for N^+ UG Polysilicon 1 sheet resistance and the value is:

$$P = 0.15203\ \mu A/^{o}C \quad (23)$$

IV. SIMULATION RESULTS

Transistors M_1 , M_2 , M_3 and M_4 have been sized from simulation using different values of *m* (2, 3, 4 and 5) in accordance with relation (22). The best results were obtained for *m* = 2 and the following transistor sizes: $L_{1,2,3,4}$=5μm, W_1=1,1μm, W_2=70μm, W_3=20μm, W_4=40μm.

In all simulated cases, we have pursued three parameters:

- *sensor sensitivity* or the percentage slope of the total-current, expressed in [%/°C], and representing a change of current versus temperature, calculated using the formula:

$$P=\frac{I_{t[120^\circ C]}-I_{t[-30^\circ C]}}{I_{t[45^\circ C]}\cdot[120^\circ C-(-30)^\circ C]}\cdot 100 \quad (24)$$

where $I_{t[-30^\circ C]}$; $I_{t[45^\circ C]}$ and $I_{t[120^\circ C]}$ represent the total-current measured at the minimum, middle and maximum temperature range.

The percentage was used to compare slopes of different cases of variation in the process without interfering with ongoing component of total-current.

- *The deviation or nonlinearity*, expressed in [%], was measured as the ΔI / I_{ideal} ratio, where ΔI is the difference between the ideal-current (as a line on graph) and total-current sensor.

- *SR parameter* was measured which indicates the minimum voltage supply of circuit (V_{DDmin}).

The results were entirely unsatisfactory (high values for the total-current) when the circuit simulation was performed using resistance R_1 of PTC type.

The simulations with ZTC-type R_1 resistance determined an increased performance in terms of the nonlinearity. It results as low as 0.52%, the percentage sensitivity is 0,1488[%/ºC], and not very great SR = 10268ppm/V to V_{DDmin}= 3.5V. The current consumption for this type of sensor has a value of 27µA at 20^{o}C.

The slope calculated when the total-current variation is in range of -30…120°C is 0.04285[µA/ºC].

Although we have a very good linearity, this case is not a viable one because the slope is much smaller than the calculated value.

Regarding the third case, when R_1 is of NTC type, the total-current temperature dependency graph is shown in Fig.4.

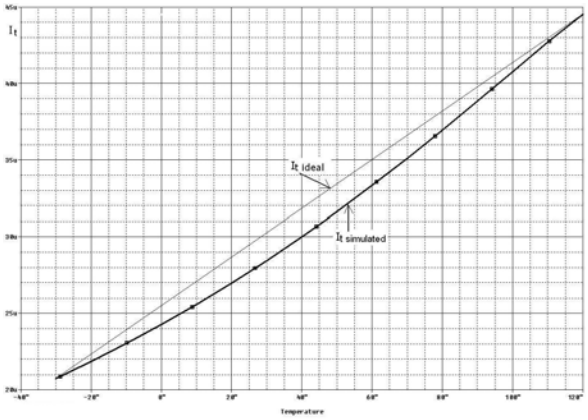

Fig. 4. Total-current variation with temperature for NTC-type R_1 resistance

The maximum percentage sensitivity in this case is obtained for m=2 and R_1=80kΩ and is 0,5146%/ºC. This type of resistance has very large square resistance, 1000Ω/□. This will lead to a small occupied-on-chip area and a low cost implementation. The total-current slope obtained by simulation is good, 0,1584µA/ºC, with an error of only 4.05%.

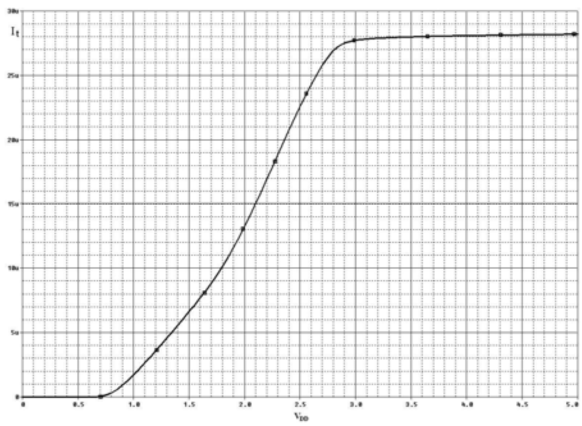

Fig.5. Total-Current dependence on the supply voltage.

In this case we have two major drawbacks: the current nonlinearity is very high (5.81%) and V_{DDmin} is quite high (3.5V) where SR is of 8830ppm/V (fig. 5).

In order address this problem, we introduce an upper resistance above the simple mirror as presented by Fig. 6.

Based on the new circuit simulation results, we conclude that R_3 placed on the right side is not a solution to address the two disadvantages.

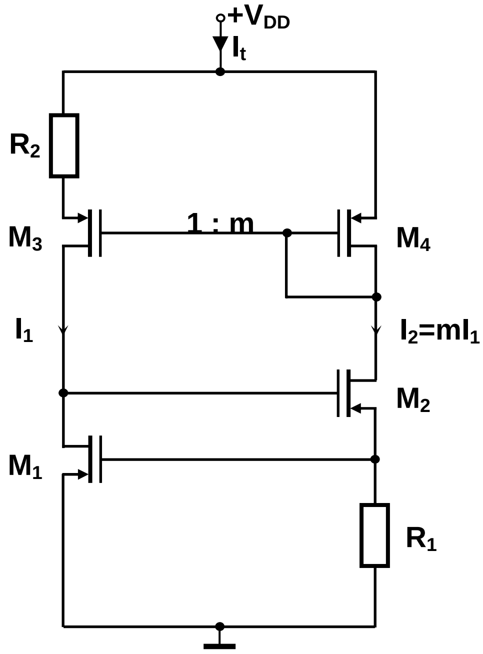

Fig.6. Proposed CMOS total-current Wilson-Widlar temperature sensor.

Alternatively, when R_2 is considered on the left side, very good linearity performance, going down to 0.47%, is obtained. Also it brings V_{DDmin} to 2.4V, with a SR=7897ppm/V measured at 3.5V.

Simulations were made with all types of resistance thermal coefficient for R_2 : positive, zero and negative and it was the best option for the type PTC, which has the value of 3.7 kΩ.

Table2: Simulation result for different type of R_2

R_2	PTC	ZTC	NTC
Percentage Slope [%/ºC]	0,5146	0,1320	0,2411
Total-current Slope[µA/ºC]	0,1584	0,0539	0,1006
Nonlinearity[%]	0,47	1,38	0,68
Current consumption [µA]	42,9	39,46	39,8
$V_{dd\ min}$ [V]	2,4	2,4	2,4

V. PROCESS VARIATIONS

For the final version of the proposed temperature sensor, simulations by varying the process, to five temperatures in the range -30 to 120 °C, were performed. We have in view the variation of percentage slope of total-current versus process and the total-current dependency on process

The simulation generated graphs, for typical parameters, the best case and worst case are depicted in Fig. 7.

Next, we managed to optimize the sensor by modifying the widths of resistors R_1 and R_2. The total variation of percentage slope of total-current versus process is now 3.66%, -1.94% for BC compared to TYP and 1.72% for WC compared to TYP.

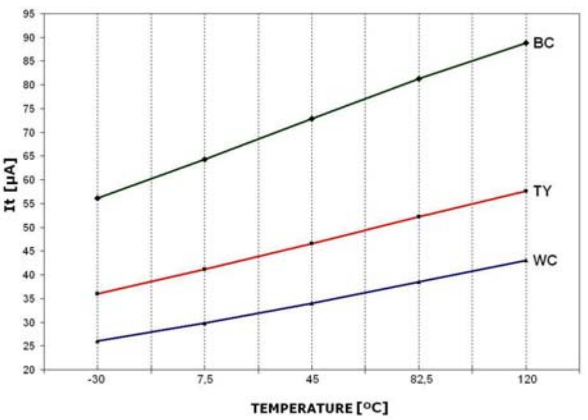

Fig. 7. Total-current dependency on process and temperature.

The Widlar-Wilson total-current temperature sensor needs trimming, which will be done with a specific circuit and a small number of bits [2], which is an advantage over the traditional approaches.

The estimated occupied-on-chip area by the temperature sensor with resistance R_1 of NTC type (with square resistance of 1000Ω/□) and the resistance R_2 of PTC type, leads to 5125µm^2 value.

Also the area can be reduced if we put another resistance of the same type with R_1 instead of PTC resistance. The resistances should have a large value of the quadratic resistance. This leads to a lower area occupied on the chip, in the detriment of the achieved performances.

VI. CONCLUSIONS

This paper present and analyse the design of a temperature sensor in the 0.35µm technology, consisting of two cross-connected classical current mirrors.

Similar performance had been achieved in the literature, but with complex circuits, occupying large areas on the chip. The main advantages of our proposed circuit occupying an area of 5125µm^2 are: relative simplicity and higher sensibility. See Tab. 3 for comparison with other approaches.

Another major advantage of this sensor is that it has an optimized percentage sensitivity. The total percentage variation of the slope with the process is very small, only 3.66%, (while process change of a resistor is ± 30%). However the disadvantage of this scheme is that it failed to optimize the total-current variation, which is yet too big.

Table3: Comparison with previous work

Approach	Process	component number	Area on chip	Sensitivity (slope)	Range	Nonlinearity	$V_{DD\,min}$
[5]	0.8 µm	27		0.7 mV/°C	-43...127 °C	0,12%	1.6V
[6]	0.1 µm	9	2800 µm^2	0.08 µV/°C	10...100 °C	3%	5V
[7]	0.8 µm	28	$9.7\cdot10^4$ µm^2	14.2 mV/°C	-43...127 °C		3V
[8]	1.2 µm	17	$2\cdot10^4$ µm^2	5.1 mV/°C	-20...100 °C	1.5%	3V
this work	0.35 µm	6	5125 µm^2	0.15 µA/°C	-40...120 °C	0.4%	2.4V

The error of 4.05% between the slope obtained by analytical way and the one obtained from simulations, the nonlinearity 0.47%, the total variation of percentage slope of total-current versus process of only 3.66% and the estimating area on chip of only 5125µm^2, are other outcomes of our designing method. The optimized sensor variant, using R_2 with positive temperature coefficient, achieved a minimum supply voltage of 2,4V and a SR=7897ppm/V at 3.5V.

REFERENCES

[1] R. Mihăescu, "First-Order Temperature – Compensated Total – Current Reference", *12th WSEAS International Conference on Circuits, Crete Island*, July 2008.
[2] H. Dong-Ok; K. Yong-Il; P. Tah-Joon; P. Heon-Chul, "A CMOS temperature sensor with calibration function using band gap voltage reference", *Sensing Technology, ICST 3rd International Conference*, pp: 496-499, 2008.
[3] M. Sasaki et at., "A temperature sensor with an inaccuracy of -1/+0.8 ºC using 90-nm 1-V CMOS for online thermal monitoring of VLSI circuits", *IEEE Trans. Semiconductor manufacturing, vol. 21, no. 2*, pp. 201–208, May 2008.
[4] M. A. P. Pertijs, "Precision Temperature Sensors in CMOS Technology", *Springer Publishing,* 2006.
[5] P. Aguirre and C. Rossi, "Architecture and cells for micropower temperature sensors", *Proc. of the X Workshop Iberchip*, Cartagena de Indias, Colombia, session 6C, March 2004..
[6] V. Székely, C. Márta, Z. Kohári, M. Rencz, "CMOS Sensors for On-Line Thermal Monitoring of VLSI Circuits", *IEEE Transactions on VLSI Systems, vol.5, no.3*, Sept. 1997, pp.270-276.
[7] C. Rossi, P. Aguirre., "Ultra-low power CMOS cells for temperature sensors", *IEEE 18th Integrated Circuits and Systems Design*, pp. 202-206, Sept. 2005.
[8] T. Ohzone, T. Sadamoto, T. Morishita, K. Komoku, T. Matsuda, H. Iwata, "A CMOS Temperature Sensor", *IEICE Trans. on Electronics, vol.E90-C, no.4*, pp.895-902, 2007.